



# Comparative Analysis of MPPT Control Techniques to Enhance Solar Energy Utilization and Convergence Time Under Varying Meteorological Conditions and Loads

Jaswant Singh<sup>1\*</sup>, S. P. Singh<sup>1</sup>, K. S. Verma<sup>2</sup> and Bhavnesh Kumar<sup>3</sup>

<sup>1</sup>Department of Electrical Engineering, Rajkiya Engineering College, Ambedkar Nagar, India, <sup>2</sup>Department of Electrical Engineering, Kamla Nehru Institute of Technology, Sultanpur, India, <sup>3</sup>Department of ICE, Netaji Subhas University of Technology, New Delhi, India

## OPEN ACCESS

### Edited by:

Shabana Urooj,  
Princess Nourah bint Abdulrahman  
University, Saudi Arabia

### Reviewed by:

Krishan Kumar,  
Dehn India, India  
Seema Kewat,  
Hong Kong Polytechnic University,  
Hong Kong SAR, China  
Mohammad Amir,  
Jamia Millia Islamia, India  
Dheeraj Joshi,  
Delhi Technological University, India

### \*Correspondence:

Jaswant Singh  
jaswant.knit2011@gmail.com

### Specialty section:

This article was submitted to  
Smart Grids,  
a section of the journal  
Frontiers in Energy Research

Received: 17 January 2022

Accepted: 23 May 2022

Published: 14 July 2022

### Citation:

Singh J, Singh SP, Verma KS and  
Kumar B (2022) Comparative Analysis  
of MPPT Control Techniques to  
Enhance Solar Energy Utilization and  
Convergence Time Under Varying  
Meteorological Conditions and Loads.  
Front. Energy Res. 10:856702.  
doi: 10.3389/fenrg.2022.856702

The electrical energy generated from solar energy photovoltaic (PV) technology is intermittent, varying, and irregular. With PV technology's limited energy conversion efficiency, it is imperative to extract the maximum of converted energy. The zero slopes of the power versus voltage curve are utilized to determine the maximum power point. Conventional algorithms provide lower convergence time along with low power oscillations. This paper proposes an adaptive perturb and observe (A-P&O) maximum power point tracking (MPPT) technique for the energy conversion system. The primary objectives of the proposed technique are to obtain a more robust, better tracking capability, improved efficiency, and fast response lesser oscillations under steady-state with a simple structure to implement. Maximum power point (MPP) tracking under varying meteorological conditions and load variations is still a challenge. The proposed P&O technique has been tested under realistic meteorological variations and load variations. The comparative evaluation of the proposed adaptive-step size A-P&O MPPT technique and other conventional techniques such as perturb and observe (P&O), incremental conductance (IC), modified P&O and fuzzy logic control (FLC) have also been performed. The performance of the proposed control technique is evaluated using a MATLAB/Simulink environment. The obtained results confirm that the proposed control technique is superior in performance as compared to the other four conventional techniques.

**Keywords:** PV array, boost converter, MPPT technique, maximum power point, meteorological conditions

## 1 INTRODUCTION

In recent years, due to the increasing demand for electricity in the domestic and industrial sectors, almost every country is struggling with an energy deficit. Consequently, continuous expansion of conventional energy generation systems to meet the demand is happening, increasing the threat to the environment in terms of carbon footprints. In addition; raw material used in conventional methods is exhausting at a rapid rate (Jiayi et al., 2008). Due to this, researchers are looking for alternate energy sources which are renewable and have a clean

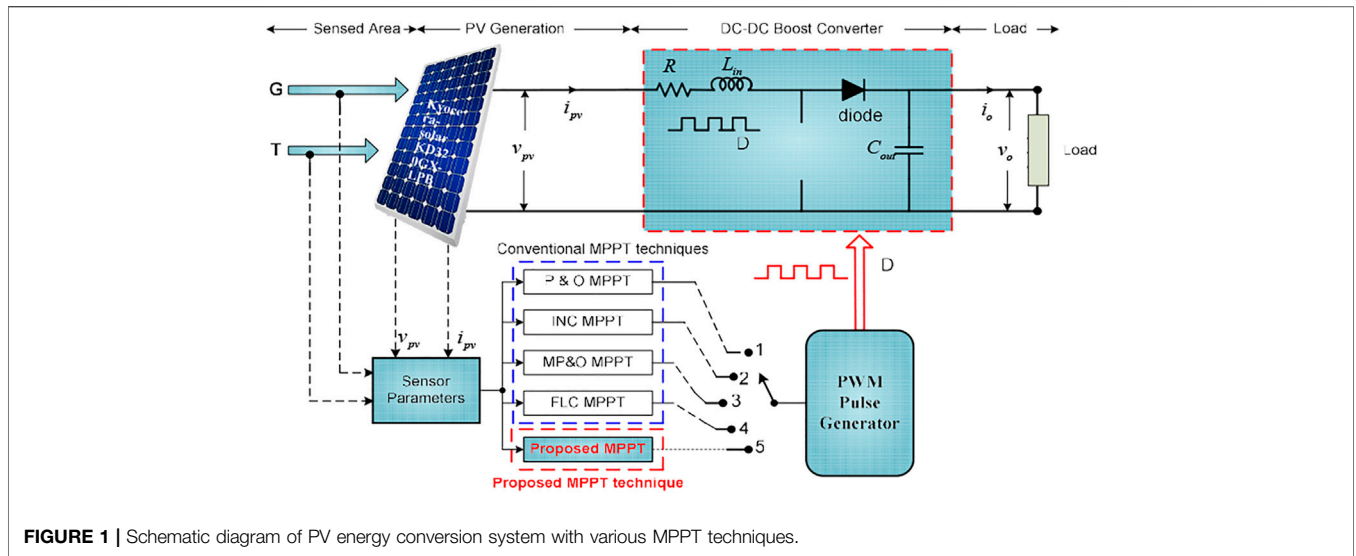


FIGURE 1 | Schematic diagram of PV energy conversion system with various MPPT techniques.

TABLE 1 | Specification parameters of Kyocera-solar KD320GX-LPB PV module and array.

Quantity	Symbols	Values
PV module		
Power at MPP	$P_{mmp}$	321 W
Voltage at MPP	$V_{mmp}$	40.1 V
Current at MPP	$I_{mmp}$	7.99 A
Short-circuit current	$i_{sc}$	8.6 A
Open circuit voltage	$V_{oc}$	49.5 V
PV array		
Power at MPP	$P_{mmp\_array}$	2,563 kW
Voltage at MPP	$V_{mmp\_array}$	320.8 V
Current at MPP	$I_{mmp\_array}$	$3,560/320.8 \approx 7.99$ A
Number of series string	$N_{ser}$	$320.8/40.1 = 8$
Number of parallel strings	$N_p$	1

TABLE 2 | The specification of electrical parameters for the boost converter.

Parameters	Symbols	Values
Boost inductor	$L_{boost}$	5.1 mH
Internal resistance	$R_{int}$	0.001 $\Omega$
Boost capacitors	$C_{boost}$	80 $\mu$ F
Boost input capacitors	$C_1$	100 $\mu$ F
Switching frequency	$f_s$	20 kHz
PV voltage range	$V_{pv}$	$320.8 \pm 8.5$ V
Load voltage range	$V_{Load}$	$500 \pm 8.5$ V

process of energy generation. Currently, renewable energy sources such as solar energy, wind energy, fuel cell, biogas, geothermal, and micro-turbine are prominent excerpts in the generation of electricity. The solar energy hypothesis is one of the most important sources of the future energy mix. Also, due to recent research and developments in the field of power

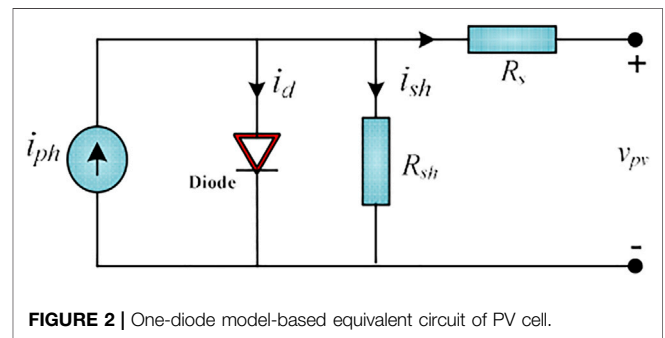
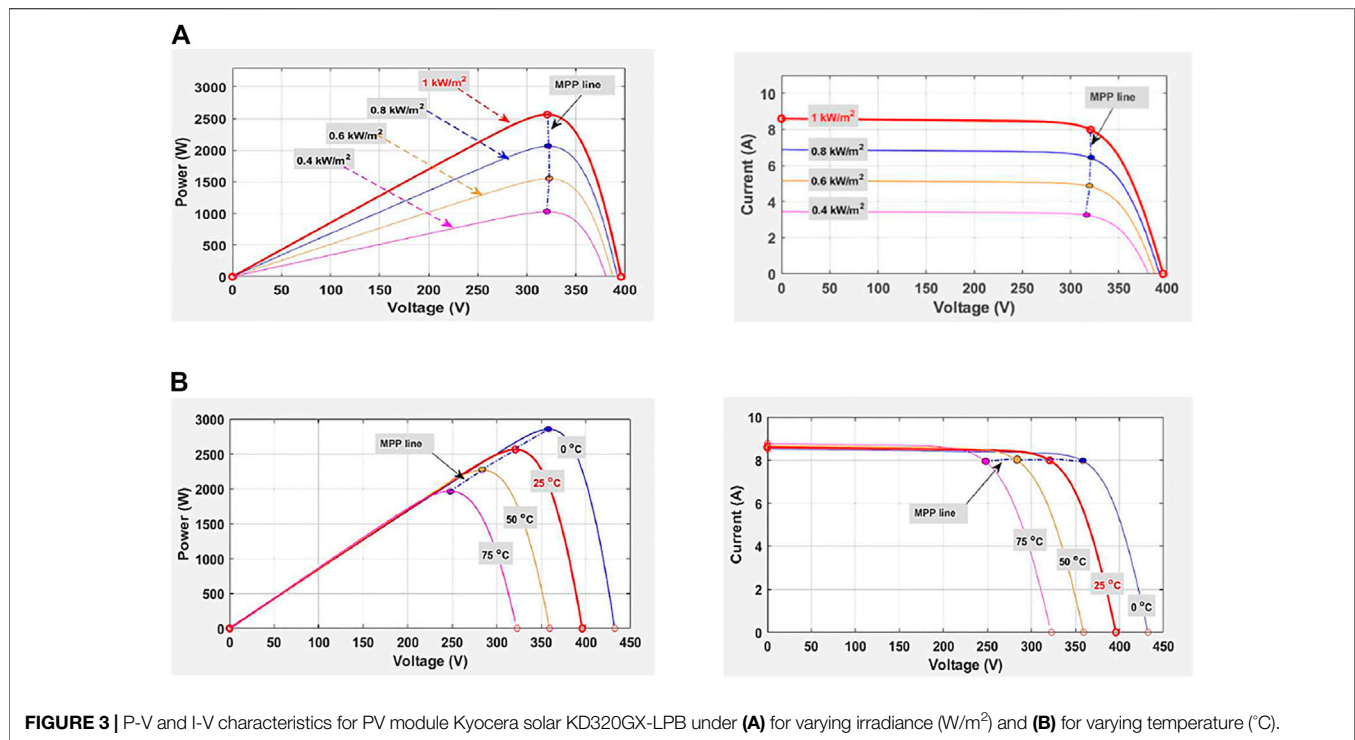


FIGURE 2 | One-diode model-based equivalent circuit of PV cell.

electronics have made solar energy more feasible for domestic and industrial applications (Dolara et al., 2009).

Systems utilizing solar energy can be classified as solar thermal systems and solar PV systems. However, photovoltaic (PV) power is most promising and beneficial because of its easy installation, pollution-free, clean with low-cost, long life, noiseless, and required low maintenance. Also, the PV market is showing a steady and sustained evolution, all over the world with rapid cost reduction and increased efficiency in technology (Mekhilef et al., 2011). However, the overall power conversion efficiency of these PV cells is low (35–40% approximately). Furthermore, exploitation of the generated energy by these PV cells is strongly affected by loading conditions. Therefore, researchers are simultaneously exploring solutions to increase power conversion efficiency and extract maximum power through the MPPT techniques. Typically, the available power from the PV array depends on irradiance level and ambient temperature whereas extracted power is dependent on loading conditions. Because of the non-linear relationship between cell voltage and current, the power available for extraction will be maximum at a certain operating point only. Furthermore, MPP varies with the variation in operating conditions of the PV system (Li, 2019; Reza Reisi et al., 2013). Therefore, it is imperative to use maximum power point tracking techniques (MPPT) to extract the



**FIGURE 3** | P-V and I-V characteristics for PV module Kyocera solar KD320GX-LPB under (A) for varying irradiance ( $W/m^2$ ) and (B) for varying temperature ( $^{\circ}C$ ).

maximum available power in every operating condition (Hlaili and Mecherqui, 2016).

Over the past decade, several reports and research articles have achieved enhanced energy conversion efficiency in PV technology using different MPPT techniques. These MPPT techniques can be divided into three types: conventional, artificial-intelligence (AI), and hybrid-based techniques. Constant voltage control (CVC) (Kumar et al., 2014; Derbeli et al., 2021), Hill-Climbing (Jordehi, 2016; Amir et al., 2017; Pavithra et al., 2021), Perturb & Observe (P&O) (Esrasm and Chapman, 2007; Yilmaz et al., 2019; Mousa et al., 2021), Sliding Mode Control (SMC) based MPPT technique (Ahmed and Salam, 2016), Incremental Conductance (IC) (Li and Wang, 2009; Kumar et al., 2014; Mamarelis et al., 2014; Bendib et al., 2015), incremental resistance (IR) based MPPT (Chauhan et al., 2020), and fractional voltage/current (Elbaset et al., 2015) are conventional techniques having less complex behavior and are easy to implement. Among these, P&O and IC algorithms are more prevalent. Second category algorithms use soft computing or artificial-intelligence (AI) based techniques namely: fuzzy logic controller (FLC) based MPPT (Saravanan and Ramesh Babu, 2016), artificial neural network (ANN) MPPT (Kottas et al., 2006), adaptive neuro-fuzzy inference system (ANFIS) based MPPT (Ben Salah and Ouali, 2011; Amara et al., 2018), particle swarm optimization (PSO) based MPPT (Algarín et al., 2017; Aouchiche et al., 2018; Wang et al., 2018) technique and evolutionary algorithms (EA) based MPPT. These intelligent techniques are suited for efficient operation in more dynamic environments to produce output with lesser steady-state oscillations, but they are more sophisticated as compared to conventional techniques requiring more resources for effective realization. In addition, several hybrid MPPT techniques using

combinations of conventional/Artificial-Intelligence (AI)/modification of conventional techniques have also been introduced to deal with dynamic and partial-shading conditions. Some of the combinations for hybrid controllers are modified P&O (Esrasm and Chapman, 2007; Bayrak and Ghaderi, 2019), PI-FLC based MPPT (Saravanan and Ramesh Babu, 2016; Eltamaly and Farh, 2019), and Neural-fuzzy logic (N-FL) based technique (Loukil et al., 2020). However, these MPPT techniques are immensely complex and expensive as compared to conventional techniques.

P&O control technique is widely used as it can be implemented with low-cost microprocessors, simple, and robust. However, the three main drawbacks of this technique: large steady-state oscillation, slow tracking response, and dependency of step dimension, make it less suited under rapidly varying meteorological conditions. Whereas, overcoming the limitations through improvement or modification in the P&O MPPT technique (Bayrak and Ghaderi, 2019) increases the complexity.

A rapid and variable step-size P&O technique that eliminates large fluctuations and slow tracking response of the conventional version. Simulations results are validated through MATLAB/Simulink model which indicates reduced steady-state oscillations, improved efficiency, and optimal power extraction. The detailed performance analysis is conducted in comparison with conventional MPPT control techniques such as P&O (Esrasm and Chapman, 2007), IC (Li and Wang, 2009), MP&O (Bayrak and Ghaderi, 2019), and FLC (Saravanan and Ramesh Babu, 2016) techniques, respectively. A white-box mathematical model has been developed using fundamental principles of PV physics and the system developed is

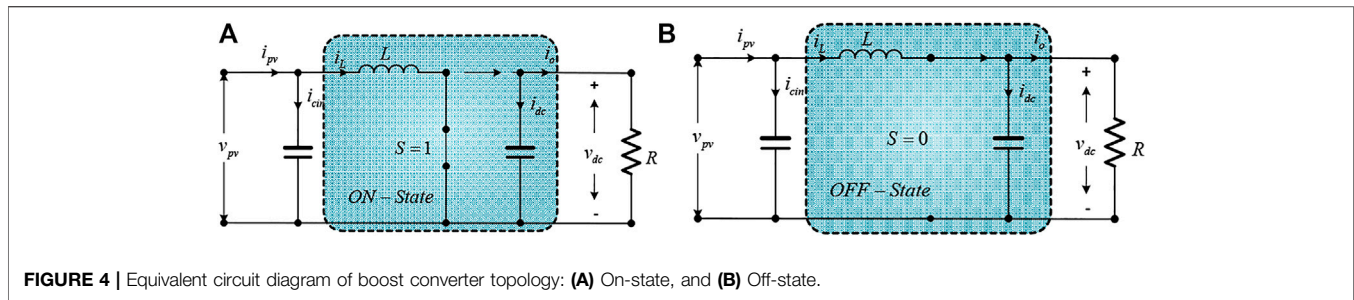


**FIGURE 4** | Equivalent circuit diagram of boost converter topology: **(A)** On-state, and **(B)** Off-state.

incorporated using a boost converter (Mekhilef et al., 2011) with a suitable duty cycle as shown in **Figure 1**.

Significant contributions of this paper are as follows:

- The developed MPPT technique is implemented and validated to extract maximum power under varying meteorological conditions and load variations.
- The performance of a PV-connected boost converter using the proposed MPPT technique gives reduced steady-state oscillation, improved efficiency, extract optimal power, and fast-tracking response.
- The proposed technique is compared with conventional techniques available in literature such as perturb and observed (P&O), incremental conductance (IC), modified P&O, and fuzzy logic control (FLC).

This paper is systematically organized as follows: **Section 2** explains an overall system configuration and mathematical model of the PV system (*i.e.*, PV array, electrical characteristics, boost converter) in detail. **Section 3** describes the comparison between the conventional and the proposed MPPT techniques. In **Section 4**, the performance investigation of the proposed MPPT and four traditional MPPT techniques are verified via simulation test results and a comparative study has been presented. Finally, concluding remarks are given in **Section 5**.

## 2 SYSTEM CONFIGURATION AND MODELING

The system under consideration consists of the following components: PV array; MPPT; boost-converter; and electric load (battery, resistive, inverter, etc.). The arrangement of the different components is depicted in **Figure 1**, which consists of a PV array, a boost converter, and an MPPT controller. The parameters and ratings of the PV panel and the boost converter are given in **Table 1** and **Table 2**, respectively.

### 2.1 Solar PV Cell

#### 2.1.1 Mathematical Modeling of PV Cell

The basic equivalent-circuit model of a solar PV cell is depicted in **Figure 2**. The exclusive goal of modeling PV cell using a one-diode represented here is to mimic the characteristics and performance of PV cells under irregular climate conditions (Pavithra et al., 2021).

The mathematical expression for solar photovoltaic cell output current can be given as:

$$i_{pv} = i_{ph} - i_d - i_{sh} \quad (1)$$

where;  $i_{pv}$  is the photovoltaic current,  $i_{ph}$  is photocurrent,  $i_d$  is diode current and  $i_{sh}$  is shunt-resistance current.

In a solar PV cell, the diode current  $i_d$  is expressed as:

$$i_d = i_{rs} \left[ \exp \left( \frac{q(V_{pv} - i_{pv}R_s)}{kT} \right) - 1 \right] \quad (2)$$

from **(Eq. 1)** and **(Eq. 2)**, the net PV current can be expressed as:

$$i_{pv} = i_{ph} - i_s \left[ \exp \left( \frac{q(V_{pv} - R_s i_{pv})}{kT N_s} \right) - 1 \right] - \frac{V_{pv} + R_s i_{pv}}{R_{sh}} \quad (3)$$

where;  $i_s$  is the saturation or leakage current of the diode,  $\mathcal{A}$  is the diode ideality factor constant,  $q$  is the electronic charge ( $q = 1.602 \times 10^{19} \text{e}^-$ ),  $k$  is the Boltzmann constant ( $k = 1.368 \times 10^{-23} \text{J/K}$ ), and  $T$  is the actual temperature (in Kelvin).

Furthermore, photocurrent  $i_{ph}$  is linearly incumbent on the solar PV radiation as well as influenced by standard test condition temperature ( $T_{STC} = T$ ) can be represented by **Eq. 4**.

$$i_{ph} = [i_{sc} + k_i(T - T_r)] \times \frac{\mathcal{G}}{\mathcal{G}_{erf}} \quad (4)$$

where,  $i_{sc}$  is the short-circuit current,  $\mathcal{G}$  is the solar radiation,  $k_i$  are the parameters of PV solar cell SC current,  $T_n$  is the reference temperature. The reverse saturation and saturation current of the photovoltaic module, which changes with the temperature can be calculated by **Eqs. 5,6**.

$$i_{rs} = \frac{i_{sc}}{\exp(qV_{pv}/kT N_s) - 1} \quad (5)$$

$$\text{and } i_s = i_{rs} \left( \frac{T}{T_n} \right)^3 \exp \left( \frac{qE_g}{kT} \left[ \frac{1}{T_n} - \frac{1}{T} \right] \right) \quad (6)$$

where  $E_g$  is the semiconductor energy bandgap,  $i_{rs}$  is the reverse saturation current at weather change conditions. PV modules are interconnected in series and parallel forming an array to deliver a sufficient amount of power to the load. Considering the scenario modified equation for the output photovoltaic current can be given **Eq. 7**.

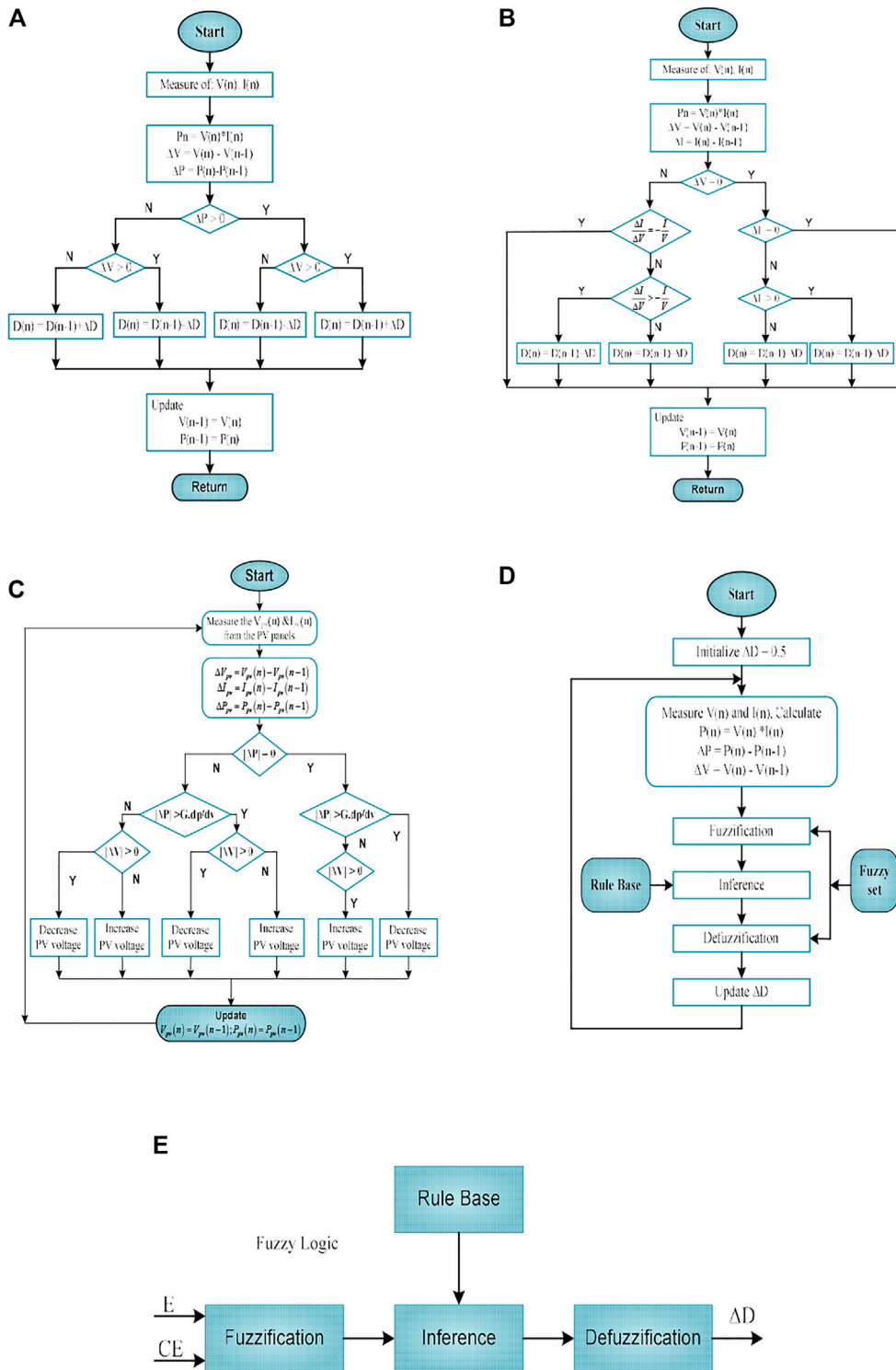


**FIGURE 5** | Flow-chart of the four conventional MPPT techniques **(A)** P&O (Esram and Chapman, 2007) **(B)** Inc Cond (Li and Wang, 2009) **(C)** MP&O (Bayrak and Ghaderi, 2019) **(D)** FLC based MPPT (Saravanan and Ramesh Babu, 2016). **(E)**. Block diagram of FL-MPPT technique.

$$\therefore i_{pv} = \mathcal{N}_p i_{ph} - \mathcal{N}_p i_s \left[ \exp \frac{q(V_{pv} - \mathcal{R}_s i_{pv})}{AkT\mathcal{N}_s} - 1 \right] - \mathcal{N}_p \frac{V_{pv} + \mathcal{R}_s i_{pv}}{\mathcal{N}_s \mathcal{R}_{sh}} \quad (7)$$

where  $\mathcal{N}_s$  represents the series-connected modules and  $\mathcal{N}_p$  represents the parallel-connected modules.

### 2.1.2 Influence of P-V and I-V Characteristics for PV Module at STC

According to standard test conditions, the irradiance and the temperature should be 1000 W/m<sup>2</sup> and 25°C, respectively. A commercially available Kyocera solar PV cell (KD320GX-LPB) is chosen for this study. Power-Voltage (P-V) and Current-Voltage (I-V) characteristics for different irradiance and temperature ( $T_{STC} = 20^\circ\text{C}$  to  $60^\circ\text{C}$  and  $G = 400 \text{ W/m}^2$  to  $1000 \text{ W/m}^2$ ) are depicted in **Figures 3A,B**.

As evident from **Figure 3**, the increase in irradiance, increases the generated power, whereas a rise in the temperature reduces it. The maximum output power ( $\mathcal{P}_{mpp}$ ) and voltage ( $V_{mpp}$ ) are extracted from the peak point of the curve under variable environmental conditions. The current ( $I_{mpp}$ ) and voltage ( $V_{mpp}$ ) at the maximum power point are also extracted from the peak point of the curve. The maximum power point of the PV system can be expressed as:

$$\mathcal{P}_{mpp} = V_{mpp} \times I_{mpp} \quad (8)$$

## 2.2 Modeling of dc/dc Boost Converter

The boost converter is a power electronic device that converts the average value of the voltage (or current) from a low level to a higher level, regulated by varying the duty cycle “D” at a high switching frequency (Mousa et al., 2021). Such a converter is one of the most extensively used non-isolated dc-dc converters in PV systems for tracking the MPP as it has many features such as high efficiency, robustness, and simple structure. The equivalent circuit topology of boost converter for both *on* and *off* switching modes in continuous mode of operation is shown in **Figure 4**.

The mathematical modeling of a boost converter in a continuous mode of conduction state can be expressed by **Eq. 9**. For ON time state:

$$\left. \begin{aligned} L \frac{di_L}{dt} &= v_{cin} - i_L \mathcal{R}_1 \\ \therefore C_{in} \frac{dv_{Cin}}{dt} &= \frac{1}{\mathcal{R}_{eq}} (v_{eq} - v_{Cin}) - i_L \\ C_0 \frac{dv_{e0}}{dt} &= -\frac{v_{e0}}{\mathcal{R}} \end{aligned} \right\} \quad (9)$$

where  $i_L$  or  $i_{pv}$  is inductor current,  $v_{cin}$  is input capacitor of voltage, and  $v_c$  or  $v_0$  is the voltage of the capacitor. Let state variables  $x_1 = i_L$  ( $i_{pv}$ ) and  $x_2 = v_c$  ( $v_0$ ), we can rewrite the state equations in state space.

$$\begin{bmatrix} \dot{x}_1 \\ \dot{x}_2 \end{bmatrix} = \begin{bmatrix} 0 & 0 \\ 0 & -\frac{1}{\mathcal{R}C} \end{bmatrix} \begin{bmatrix} x_1 \\ x_2 \end{bmatrix} + \begin{bmatrix} 1/\mathcal{L} \\ 0 \end{bmatrix} v_{pv} \quad (10)$$

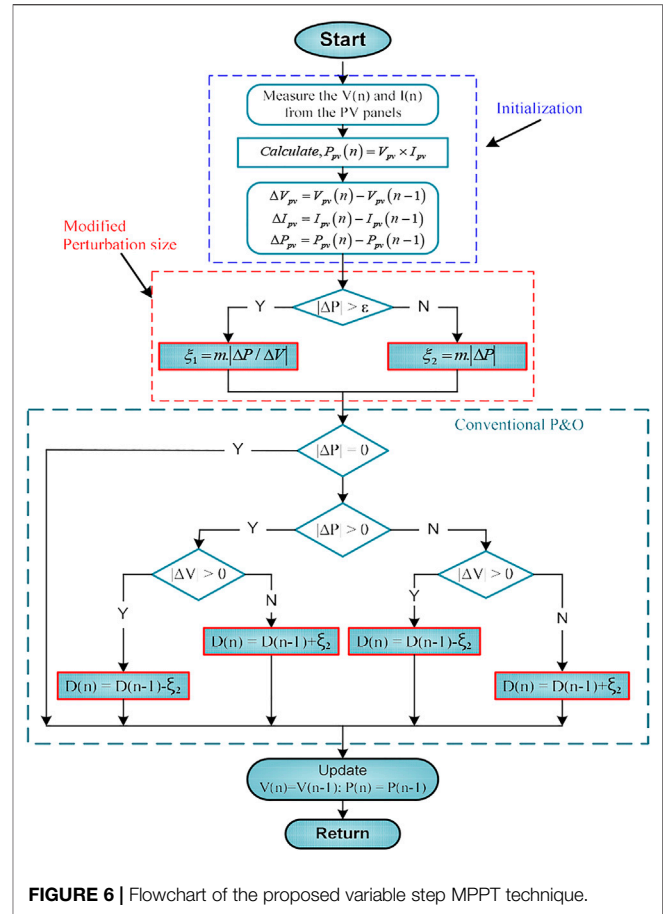


**FIGURE 6** | Flowchart of the proposed variable step MPPT technique.

at OFF time state: when the  $s = 0$ , the simplified circuit can be represented by the state equations which are as follows:

$$\left. \begin{aligned} \mathcal{L} \frac{di_L}{dt} &= v_{pv} - v_c \\ C \frac{dv_C}{dt} &= i_L - \frac{v_C}{\mathcal{R}} \end{aligned} \right\} \quad (11)$$

in the state-space, the equation is:

$$\begin{bmatrix} \dot{x}_1 \\ \dot{x}_2 \end{bmatrix} = \begin{bmatrix} 0 & -\frac{1}{\mathcal{L}} \\ \frac{1}{C} & -\frac{1}{\mathcal{R}C} \end{bmatrix} \begin{bmatrix} x_1 \\ x_2 \end{bmatrix} + \begin{bmatrix} 1/\mathcal{L} \\ 0 \end{bmatrix} v_{pv} \quad (12)$$

from the state-space matrices in **Eqs. 10–12** are obtained as:

$$[A] = [A_1] \times D + [A_2] \times (1 - D)$$

from the above state-space model of the T.F. is  $V_0(s)/d(s)$ :

$$\frac{V_0(s)}{d(s)} = C(|sI - A|)^{-1} [(A_1 - A_2)X + (B_1 - B_2)V_i] + [C_1 - C_2]X \quad (13)$$

$$\text{and } \frac{V_0(s)}{d(s)} = \frac{V_i \left[ \left( \frac{1}{\mathcal{L}C} \right) - \left( \frac{s}{\mathcal{R}C(1-D)^2} \right) \right]}{\left( s^2 + \frac{s}{\mathcal{R}C} + \frac{(1-D)^2}{\mathcal{L}C} \right)} \quad (14)$$

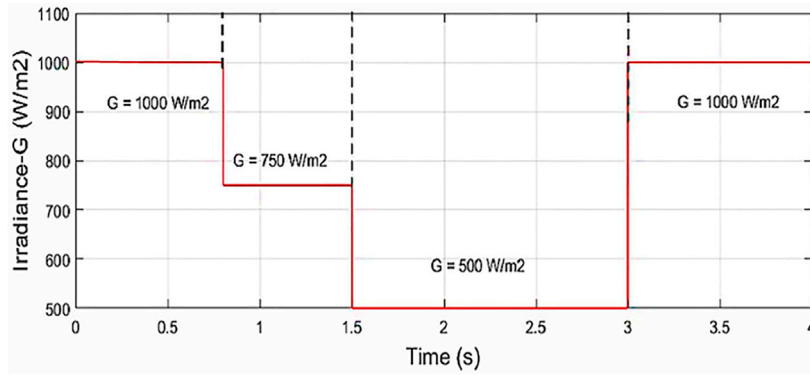


FIGURE 7 | Irradiance pattern for Scenario-I.

where  $A_{11}$  is equal to the state matrix for  $T_{on}$  time and  $A_2$  is equal to the state matrix for  $T_{off}$  period,  $V_o$  is the output voltage.

### 3 PROPOSED MPPT CONTROL TECHNIQUE

An MPPT technique is a very vital part of any solar PV system. It is employed to extract maximum power under varying meteorological conditions such as ambient temperature, irradiance, and partial shading conditions. In this paper, the performance of the conventional MPPT techniques is compared to the proposed modified perturb & observe (P&O) MPPT. A schematic of the test setup for the proposed as well as convenient technique consisting of 2.56 kW PV array is shown in Figure 1.

#### 3.1 Conventional MPPT Control Techniques

##### 3.1.1 Perturb and Observe (P&O) MPPT

The P&O technique is one of the simplest and most widely employed techniques for the control of power modulators in PV systems, because of its easy implementation in a low-cost system (Yilmaz et al., 2019). A conventional P&O algorithm can be installed with a perturbation mechanism to increase or decrease the reference voltage or current via a boost converter duty cycle ( $D$ ) so that it can detect the MPP even during changing weather conditions. Therefore, the differential changes at the output of the PV array power with respect to the instantaneous output values; otherwise, the value (voltage or current) is decreased (Esrarn and Chapman, 2007). The flow-chart shown in Figure 5A depicts the step-by-step implementation of the conventional P&O control technique by utilizing the Eq. 15.

$$\left. \begin{array}{l} dp_{pv} > 0 \text{ and } dv_{pv} > 0, \text{ left of MPP} \\ dp_{pv} > 0 \text{ and } dv_{pv} < 0, \text{ right of MPP} \\ dp_{pv} < 0 \text{ and } dv_{pv} > 0, \text{ right of MPP} \\ dp_{pv} < 0 \text{ and } dv_{pv} < 0, \text{ left of MPP} \\ dp_{pv} = 0 \text{ and } dv_{pv} = 0, \text{ at MPP} \end{array} \right\} \quad (15)$$

The conventional approach uses selected fixed step-size change in the duty cycle ( $\Delta D$ ), it is responsible for the

accuracy and speed of that system. However, the main drawbacks of this technique are large steady-state oscillation, slow tracking response, and dependency of step dimension about MPP, and less suited for variable meteorological conditions (Yilmaz et al., 2019; Mousa et al., 2021).

##### 3.1.2 Incremental Conductance (IC) MPPT

The incremental conductance control technology utilizes the information of the slope of the power curve, which will be zero at the MPP (Li and Wang, 2009). As depicted in Figure 5B, the derivative is positive on the left side, and negative on the right side of the MPP. The maximum output power available can be calculated as:

$$\mathcal{P}_{pvm} = v_{pvm} \times i_{pvm} \quad (16)$$

Differentiating Eq. 16 with respect to photovoltaic voltage, we get,

$$\frac{d\mathcal{P}_{pv}}{dv_{pv}} = \frac{d}{dv} (v_{pv}, i_{pv}) = v_{pv} \frac{di_{pv}}{dv_{pv}} + i_{pv} \frac{dv_{pv}}{dv_{pv}} = \left( \frac{di_{pv}}{dv_{pv}} + \frac{i_{pv}}{v_{pv}} \right) \quad (17)$$

at MPP, as  $dp_{pv}/dv_p = 0$  at Eq. 17 become,

$$\frac{i_{pv}}{v_{pv}} + \frac{di_{pv}}{dv_{pv}} = 0 \Rightarrow \frac{di_{pv}}{dv_{pv}} = -\frac{i_{pv}}{v_{pv}} \quad (18)$$

We define the change in instantaneous output conductance ( $G = i_{pv}/v_{pv}$ ) and incremental conductance is  $iG = di_{pv}/dv_{pv}$ . If the conductance ( $G$ ) is negative of incremental conductance ( $iG$ ) array delivers the maximum of available power and operates at MPP (Mamarelis et al., 2014). The tracking the MPP requires the following updating rules in Eq. 19 as follows:

$$\left\{ \begin{array}{l} \frac{d\mathcal{P}_{pv}}{dv_{pv}} > 0; \text{ if } \frac{i_{pv}}{v_{pv}} > -\frac{di_{pv}}{dv_{pv}} \text{ left side of MPP} \\ \frac{d\mathcal{P}_{pv}}{dv_{pv}} = 0; \text{ if } \frac{i_{pv}}{v_{pv}} > -\frac{di_{pv}}{dv_{pv}} \text{ at MPP} \\ \frac{d\mathcal{P}_{pv}}{dv_{pv}} < 0; \text{ if } \frac{i_{pv}}{v_{pv}} > -\frac{di_{pv}}{dv_{pv}} \text{ right side of MPP} \end{array} \right. \quad (19)$$

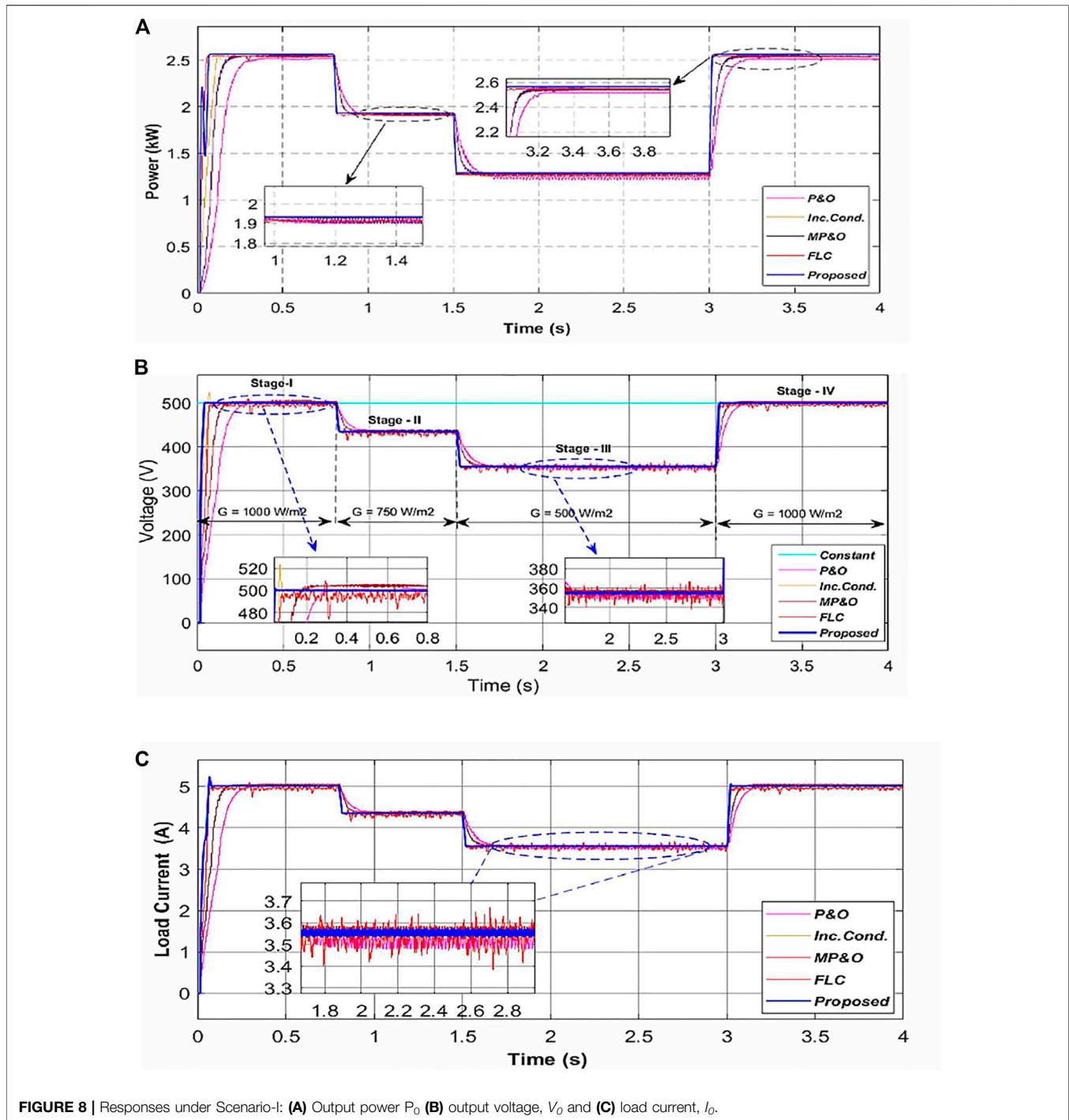


**FIGURE 8 |** Responses under Scenario-I: (A) Output power  $P_0$  (B) output voltage,  $V_0$  and (C) load current,  $I_0$ .

### 3.1.3 Modified Perturb and Observe (MP&O) MPPT

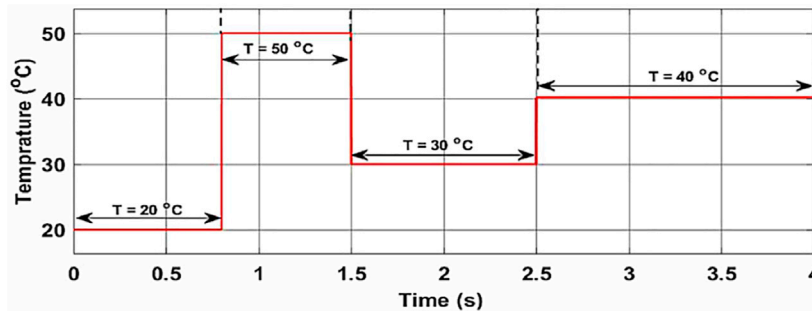
In this approach, the variable step size is considered in place of the fixed step size in the perturbation cycle. The conventional P&O technique is not capable to confer adequate response and tracking accuracy for both steady-state and dynamic conditions due to fixed step-size. If the step-size is kept large to achieve the rapid dynamic response, then the spacious oscillations around the MPP causing a loss of productive power will occur. Therefore, to

overcome this drawback a modified P&O technique was proposed by (Safari and Mekhilef, 2011; Abo-Al-Ez et al., 2020; Jana et al., 2020). **Figure 5C** shows the flowchart of the modified P&O technique depicting the strategy. It is seen from the figure that when  $|\Delta P| > P_{ref}$ , the perturbation size of the step is  $V_{stp1}$  and when  $|\Delta P| < P_{ref}$ , the perturbing size of the step is  $V_{stp2}$ . This feature makes it superior to the conventional perturb and observe MPPT techniques. Although the main drawbacks of

**TABLE 3** | Performance comparison analysis of simulation results validated under scenario-I.

MPPTs ↓	Rise time (m-sec.)				Power output (kW)				Efficiency (%)			
	$t_{rS11}$	$t_{rS12}$	$t_{rS13}$	$t_{rS14}$	$P_{0\_S11}$	$P_{0\_S12}$	$P_{0\_S13}$	$P_{0\_S14}$	$\eta_{S11}$	$\eta_{S12}$	$\eta_{S13}$	$\eta_{S14}$
P&O	301	160	161	290	2.53	1.923	1.276	2.53	98.9	98.9	98.9	98.9
Inc Cond	121	102	99.9	136	2.51	1.912	1.272	2.51	97.9	98.4	98.6	98.0
MP&O	200	145	140	185	2.54	1.936	1.284	2.54	99.4	99.6	99.6	99.4
FLC	40.1	40.0	39.8	39.8	2.54	1.932	1.282	2.54	99.3	99.4	99.4	99.3
Proposed	<b>39.9</b>	<b>35.0</b>	<b>35.1</b>	<b>35.6</b>	<b>2.55</b>	<b>1.936</b>	<b>1.285</b>	<b>2.55</b>	<b>99.6</b>	<b>99.6</b>	<b>99.6</b>	<b>99.6</b>

The bold values in Tables 3 emphasizes for proposed MPPT Technique.

**FIGURE 9** | Temperature pattern for Scenario-II.

this technique are large steady-state oscillation, slow tracking convergence, and dependency of step dimension at MPP. That builds it less suited for variable meteorological conditions on using the biggest perturbation size of steps. The MPP is reached rapidly, but the power loss due to perturbation in steady-state oscillation will also increase. The power deficit from the steady-state perturbation can be reduced with a small perturbations step but this will slow down the tracking speed.

### 3.1.4 Fuzzy Logic Controller (FLC) Based MPPT

Fuzzy logic is a soft computing (SC) technique (Saravanan and Ramesh Babu, 2016). It is among the most effective control techniques. It uses the concept of multiple rules and multiple variables ranging between entirely false and entirely true. It consists of an estimate that maps the input values to the output values derived from the IF-THEN rule. It effectively distributes with the non-linear I-V curve of the photovoltaic system which operated at a membership function instead of a mathematical module. FLC has fuzzification, inference-mechanism, defuzzification, and rule-based look-up table as main components. The flowchart of the FLC-based MPPT is depicted in **Figure 5D**. Moreover, FLC-based MPPTs usually have two inputs and one output, as shown in the **Figure 5E**. The input variables are error  $[E(n)]$  and change in error  $[CE(n)]$ , which are computed as below.

$$E(n) = \frac{\Delta \mathcal{P}}{\Delta \mathcal{V}} = \frac{\mathcal{P}(n) - \mathcal{P}(n-1)}{\mathcal{V}(n) - \mathcal{V}(n-1)} \quad (20)$$

$$CE(n) = E(n) - E(n-1) \quad (21)$$

where  $\mathcal{P}(n)$  and  $\mathcal{V}(n)$  are the immediate power and voltage of the PV system at  $n$ th sample time, whereas  $(n-1)$  indicates the value at the previous sample time.

The output variable usually changes with the change in duty ratio ( $\Delta \mathcal{D}$ ) of the boost converter, which offers rapid convergence, maintains non-linearity, and acts in exact inputs (more details can be found in Ben Salah and Ouali (2011) and Amara et al. (2018).

$$\Delta \mathcal{D}(n) = \frac{\sum_{j=1}^n \mu(\Delta \mathcal{D}_j(n)) - \Delta \mathcal{D}_j(n)}{\sum_{j=1}^n \mu(\Delta \mathcal{D}_j(n))} \quad (22)$$

The FLC output that is a change in duty ratio  $\Delta \mathcal{D}(n)$  is used to compute the final duty ratio  $\mathcal{D}(n)$  as given in **Eq. 23**:

$$\mathcal{D}(n) = \mathcal{D}(n-1) + \Delta \mathcal{D}(n) \quad (23)$$

Although the main drawbacks are that it operates at input and output membership functions instead of a mathematical model based on the experience and brief information about the operating system. Therefore, to overcome these shortcomings, we have proposed a novel MPPT technique, which is explained in **Section 3.2**.

## 3.2 Proposed Variable Step Efficient Modified P&O MPPT Technique

According to the available literature, conventional MPPT techniques described in **Section 3.1** is not capable to confer fast response and accurate tracking around MPP. This is mainly due to fixed step-size perturbation. If the step-size is kept large to achieve the rapid dynamic

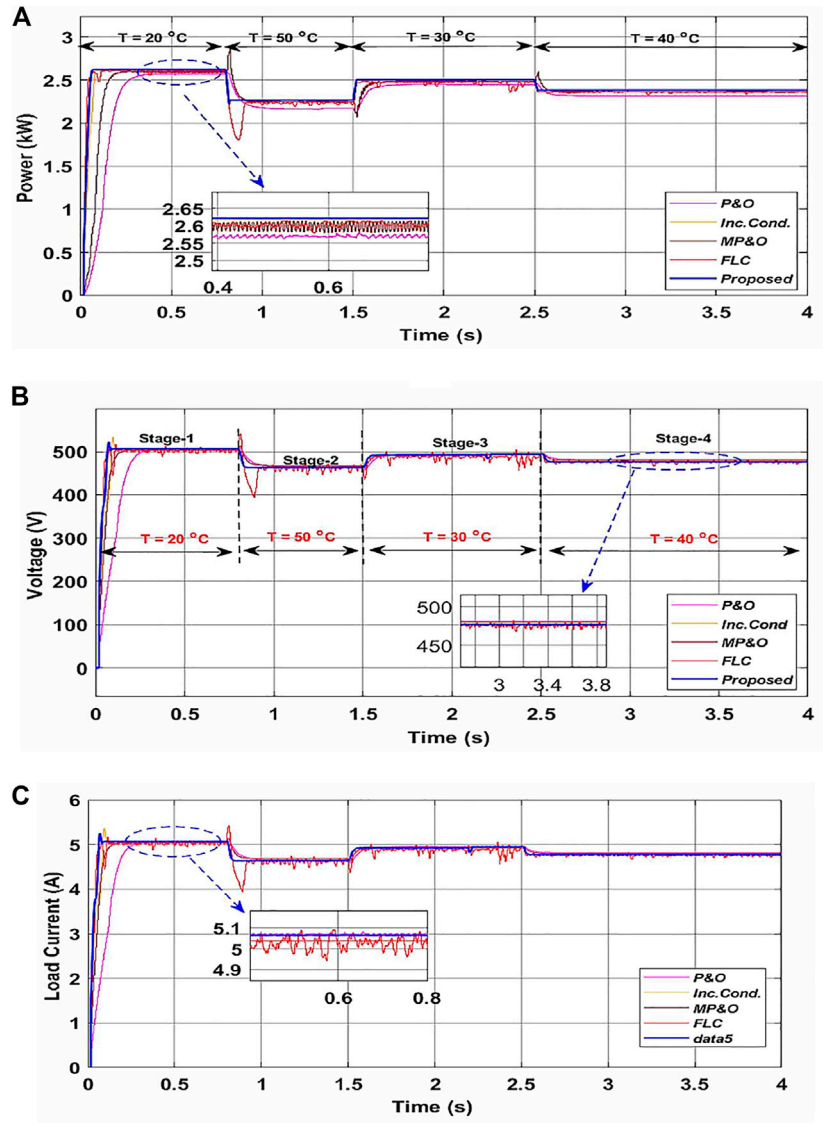


FIGURE 10 | Responses under Scenario-II: (A) Output power,  $P_o$  (B) output voltage,  $V_o$  and (C) output current,  $I_o$ .

TABLE 4 | Performance comparison analysis of simulation results validated under scenario-II.

Parameters	Rise time (m-sec)				Power output (kW)				Efficiency (%)			
	$t_{rS21}$	$t_{rS22}$	$t_{rS23}$	$t_{rS24}$	$P_{o\_S21}$	$P_{o\_S22}$	$P_{o\_S23}$	$P_{o\_S24}$	$\eta_{S21}$	$\eta_{S22}$	$\eta_{S23}$	$\eta_{S24}$
MPPTs ↓												
P&O	300	168	168	120	2.579	2.232	2.471	2.354	98.3	98.4	98.6	98.6
IncCond	119	101	99.2	90.2	2.570	2.231	2.463	2.349	98.0	98.4	99.3	98.4
MP&O	196	140	135	110	2.611	2.257	2.494	2.376	99.5	99.5	99.6	99.5
FLC	40.1	39.8	39.5	39.4	2.609	2.255	2.493	2.375	99.5	99.4	99.5	99.5
Proposed	<b>40.0</b>	<b>20.5</b>	<b>20.4</b>	<b>20.4</b>	<b>2.612</b>	<b>2.259</b>	<b>2.495</b>	<b>2.377</b>	<b>99.6</b>	<b>99.6</b>	<b>99.6</b>	<b>99.6</b>

The bold values in Tables 4 emphasizes for proposed MPPT Technique.

response, then large oscillations around the MPP will increase causing a loss of output power. Therefore, to overcome these drawbacks, proposed a new variable step-size of efficient

modified P&O (EM-PO) MPPT technique is used to eliminate these problems. According to research gaps, a novel MPPT technique is proposed in this paper, whose

**TABLE 5 |** Performance comparison analysis of simulation results validated under scenario-III.

Parameters	Resposne time (ms)				Power ouput (kW)				Efficiency (%)			
	$t_{rS31}$	$t_{rS32}$	$t_{rS33}$	$t_{rS34}$	$P_{0\_S31}$	$P_{0\_S32}$	$P_{0\_S33}$	$P_{0\_S34}$	$\eta_{S31}$	$\eta_{S32}$	$\eta_{S33}$	$\eta_{S34}$
MPPTs ↓	290	0.32	00.0	00.0	2.537	2.538	2.537	2.537	98.9	98.9	98.9	99.9
P&O	118	99.2	99.2	99.2	2.535	2.536	2.535	2.535	98.9	98.9	90.9	98.9
Inc Cond	190	140	140	140	2.551	2.555	2.551	2.551	99.5	99.5	99.5	98.5
FLC	40.0	39.5	39.5	39.5	2.550	2.554	2.550	2.550	99.5	99.5	99.5	99.5
Proposed	<b>39.9</b>	<b>20.5</b>	<b>20.5</b>	<b>20.5</b>	<b>2.553</b>	<b>2.554</b>	<b>2.553</b>	<b>2.554</b>	<b>99.6</b>	<b>99.6</b>	<b>99.6</b>	<b>99.6</b>

The bold values in Tables 5 emphasizes for proposed MPPT Technique.

**TABLE 6 |** Overall performance comparison under scenario-I, II and III.

Meteorological cond	Scenario-I				Scenario-II				Scenario-III			
	S <sub>11</sub>	S <sub>12</sub>	S <sub>13</sub>	S <sub>14</sub>	S <sub>21</sub>	S <sub>22</sub>	S <sub>23</sub>	S <sub>24</sub>	S <sub>31</sub>	S <sub>32</sub>	S <sub>33</sub>	S <sub>34</sub>
Output load voltage (V)												
P&O	498.8	436.7	354.8	498.7	506.8	468.2	496.3	484.1	449.2	504.9	436.8	478.5
Inc Cond	497.5	435.5	355.9	497.4	506.2	469.5	495.3	483.5	449.0	503.5	436.6	479.3
MP&O	502.9	437.2	356.8	502.8	509.2	469.8	499.1	489.9	449.8	504.9	437.2	480.2
FLC	499.9	434.5	356.9	499.8	508.7	470.1	499.3	489.2	450.1	505.1	437.1	480.1
Proposed MPPT	<b>501.5</b>	<b>436.1</b>	<b>358.4</b>	<b>501.5</b>	<b>509.5</b>	<b>470.1</b>	<b>499.9</b>	<b>489.9</b>	<b>451.4</b>	<b>505.5</b>	<b>437.5</b>	<b>480.0</b>
Output load current (A)												
P&O	5.08	4.38	3.59	5.08	5.08	4.76	4.97	4.86	5.64	5.03	5.80	5.29
Inc Cond	5.09	4.39	3.58	5.09	5.08	4.75	4.97	4.86	5.65	5.04	5.80	5.28
MP&O	5.09	4.40	3.59	5.09	5.12	4.80	4.99	4.85	5.67	5.06	5.83	5.31
FLC	5.07	4.44	3.60	5.07	5.11	4.79	4.99	4.85	5.67	5.06	5.83	5.31
Proposed MPPT	<b>5.10</b>	<b>4.43</b>	<b>3.59</b>	<b>5.09</b>	<b>5.12</b>	<b>4.80</b>	<b>4.99</b>	<b>4.85</b>	<b>5.65</b>	<b>5.05</b>	<b>5.83</b>	<b>5.32</b>
Output power (kW)												
P&O	2.536	1.923	1.276	2.535	2.536	2.232	2.471	2.354	2.537	2.538	2.537	2.537
Inc Cond	2.511	1.912	1.272	2.512	2.511	2.231	2.463	2.349	2.535	2.536	2.535	2.535
MP&O	2.549	1.936	1.284	2.548	2.549	2.257	2.494	2.376	2.551	2.555	2.551	2.551
FLC	2.547	1.932	1.282	2.547	2.547	2.255	2.493	2.375	2.550	2.554	2.550	2.550
Proposed MPPT	<b>2.554</b>	<b>1.936</b>	<b>1.285</b>	<b>2.554</b>	<b>2.612</b>	<b>2.259</b>	<b>2.495</b>	<b>2.377</b>	<b>2.553</b>	<b>2.554</b>	<b>2.553</b>	<b>2.554</b>
Dynamic efficiency (%)												
P&O	98.95	98.97	98.99	98.90	98.38	98.45	98.68	98.65	98.99	98.98	98.98	99.98
Inc Cond	97.97	98.40	98.68	98.01	98.02	98.41	99.36	98.44	98.90	98.94	90.90	98.90
MP&O	99.45	99.64	99.61	99.42	99.58	99.58	99.61	99.59	99.54	99.54	99.54	98.54
FLC	99.38	99.44	99.45	99.38	99.50	99.48	99.56	99.53	99.50	99.49	99.50	99.50
Proposed MPPT	<b>99.65</b>	<b>99.64</b>	<b>99.68</b>	<b>99.65</b>	<b>99.62</b>	<b>99.64</b>	<b>99.64</b>	<b>99.65</b>	<b>99.64</b>	<b>99.66</b>	<b>99.62</b>	<b>99.64</b>
Rise Time (ms)												
P&O	301	160	161	290	300	168	168	120	290	0.32	00.0	00.0
Inc Cond	121	102	99.9	136	119	101	99.2	90.2	118	99.2	99.2	99.2
MP&O	200	145	140	185	196	140	135	110	190	140	140	140
FLC	40.1	40.0	39.8	39.8	40.1	39.8	39.5	39.4	40.0	39.5	39.5	39.5
Proposed MPPT	<b>35.8</b>	<b>35.0</b>	<b>35.1</b>	<b>35.6</b>	<b>39.1</b>	<b>20.5</b>	<b>20.4</b>	<b>20.4</b>	<b>39.8</b>	<b>20.5</b>	<b>20.5</b>	<b>20.5</b>
Ripple power (kW)												
P&O	0.027	0.020	0.013	0.028	0.043	0.035	0.033	0.032	0.026	0.025	0.026	0.026
Inc Cond	0.030	0.031	0.017	0.051	0.052	0.036	0.041	0.037	0.028	0.027	0.028	0.028
MP&O	0.016	0.007	0.005	0.015	0.011	0.010	0.010	0.010	0.012	0.008	0.012	0.012
FLC	0.014	0.011	0.007	0.016	0.013	0.012	0.011	0.011	0.013	0.009	0.013	0.013
Proposed MPPT	<b>0.009</b>	<b>0.007</b>	<b>0.004</b>	<b>0.009</b>	<b>0.010</b>	<b>0.007</b>	<b>0.009</b>	<b>0.009</b>	<b>0.010</b>	<b>0.009</b>	<b>0.009</b>	<b>0.009</b>

Note (Stages: S<sub>n1</sub>, S<sub>n2</sub>, S<sub>n3</sub>, S<sub>n4</sub> and Scenario first, second, third under varying irradiance, temperature, load).

The bold values in Tables 6 emphasizes for proposed MPPT Technique.

operation could be depicted as follows: if the variable power  $|\Delta\check{P}|$  is the greater than diminutive value  $\epsilon$  (threshold of power), the perturbing size of the step is  $\xi_1$ ; if the variable power  $|\Delta\check{P}|$  is the less than diminutive value  $\epsilon$  (threshold of power), the perturbing size of step is  $\xi_2$ , here  $\epsilon$ , maximum power assumed which is a small change in irradiance. The

flowchart proposed a variable step-size EM-PO MPPT technique as depicted in **Figure 6**. The variable step-size is calculated using **Eq. 24**.

$$\check{D}(n) = \check{D}(n - 1) \pm \check{\xi}_1 \tag{24}$$

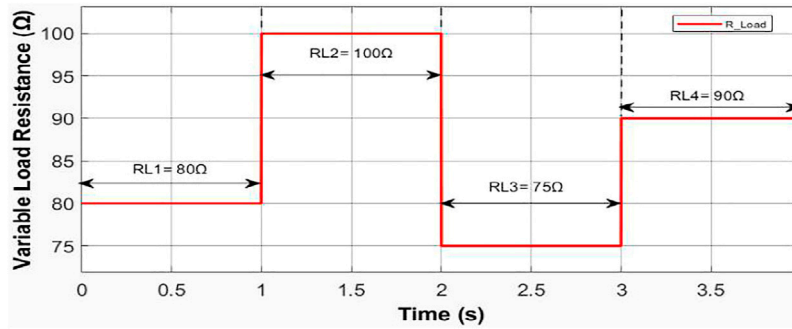


FIGURE 11 | Load variations pattern for Scenario-III.

where  $\check{D}(n)$  is the actual duty cycle,  $\check{D}(n-1)$  is the previous value of the actual duty cycle at  $n$ th sample time,  $\check{\xi}_1 = m \cdot |\Delta\check{P}/\Delta\check{V}|$  is the perturbing variable power steps and stepping factor (Kumar et al., 2014; Mamarelis et al., 2014). The variable step-size is calculated from the function of the variable power and voltage as given Eqs 25–27.

$$\check{D}(n) = \check{D}(n-1) \pm \check{\xi}_2 \quad (25)$$

$$\Delta\check{P} = \check{P}(n) - \check{P}(n-1) \quad (26)$$

$$\Delta\check{V} = \check{V}(n) - \check{V}(n-1) \quad (27)$$

where  $\Delta\check{P}$  is the power variables adjusted automatically against the irradiance changes,  $\Delta\check{V}$  is the voltage step variation to given irradiation and cell temperature conditions at  $n$ th sample time, respectively. The output steps of a proposed variable step of efficient MPO maximum power point tracking technique are given as follows:

$$\begin{aligned} \check{D}_{\xi_1}(n) &= \check{D}(n-1) \pm m \cdot \left| \frac{\Delta\check{P}}{\Delta\check{V}} \right| \\ &= \check{D}(n-1) \pm m \cdot \left| \frac{\check{P}(n) - \check{P}(n-1)}{\check{V}(n) - \check{V}(n-1)} \right| \end{aligned} \quad (28)$$

$$\check{D}_{\xi_2}(n) = \check{D}(n-1) \pm m \cdot |\Delta\check{P}| = \check{D}(n-1) \pm m \cdot |\check{P}(n) - \check{P}(n-1)| \quad (29)$$

here,  $\check{\xi}_1 = m \cdot |\Delta\check{P}/\Delta\check{V}|$  and  $\check{\xi}_2 = m \cdot |\Delta\check{P}|$  are the automatic step changes of the PV system under variable changes,  $m$  is the scaling or stepping factor for automatically adjusted at step-size, respectively. The calculation of the scaling factor ( $m$ ) is expressed in Eq. 30 which is as follows:

$$\begin{cases} m \cdot \left| \frac{\Delta\check{P}}{\Delta\check{V}} \right|_{\check{\xi}_{1min}} \geq \check{\xi}_{1min} \\ m \cdot |\Delta\check{P}|_{\check{\xi}_{2max}} \leq \check{\xi}_{2max} \end{cases} \quad (30)$$

where the predefined value of  $\check{\xi}_{2max}$  has a higher limit for the actual duty-cycle. After rearranging (Eq. 17), the slope  $d\check{P}/d\check{V}$  is given as:

$$\left| \frac{d\check{P}}{d\check{V}} \right| = I + \frac{d\check{I}}{d\check{V}} \check{V} \triangleq I + \frac{\Delta\check{I}}{\Delta\check{V}} \check{V} \quad (31)$$

The effective power  $|\Delta\check{P}|$  of perturbing and observing technique is,

$$|\Delta\check{P}| = (I + \Delta\check{I})(\check{V} + \Delta\check{V}) - I\check{V} = \left| \frac{d\check{P}}{d\check{V}} \right| \cdot \Delta\check{V} + \Delta\check{I} \cdot \Delta\check{V} \quad (32)$$

### 3.2.1 Control Strategy of Proposed Technique

The overall performance of proposed the new MPPT technique A- P&O is designed using the following steps:

- Step-1: Measuring initialize of  $n$ th values are  $\check{V}(n)$  and  $\check{I}(n)$  by sampling. After that calculation, the  $n$ th value of power  $\check{P}(n)$  is measured by product of  $\check{V}(n)$  and  $\check{I}(n)$  using Eq. 16, respectively.
- Step 2: To calculate the  $|\Delta\check{P}| = \check{P}(n) - \check{P}(n-1)$  and  $|\Delta\check{V}| = \check{V}(n) - \check{V}(n-1)$ , respectively.
- Step 3: If the variable power  $|\Delta\check{P}|$  is larger than the diminutive value  $\epsilon$ , the perturbing size of step is  $\xi_1$ . The  $\xi_1$  is calculated in terms of Eq. 28 and sent to pulse-generator to drive the switching of dc-dc converter topology.
- Step 4: If the variable power  $|\Delta\check{P}|$  is less than the diminutive value  $\epsilon$ , the perturbing step-size is  $\xi_2$ . The  $\xi_2$  is calculated in terms of Eq. 29 and sent to same of above, it is indicating that the meteorological condition such as irradiance and temperature has rapidly changed.
- Step 5: Update the best individual solution envisaged by each  $\check{V}(n-1) = \check{V}(n)$ ;  $\check{I}(n-1) = \check{I}(n)$  and their included duty cycle at MPP.

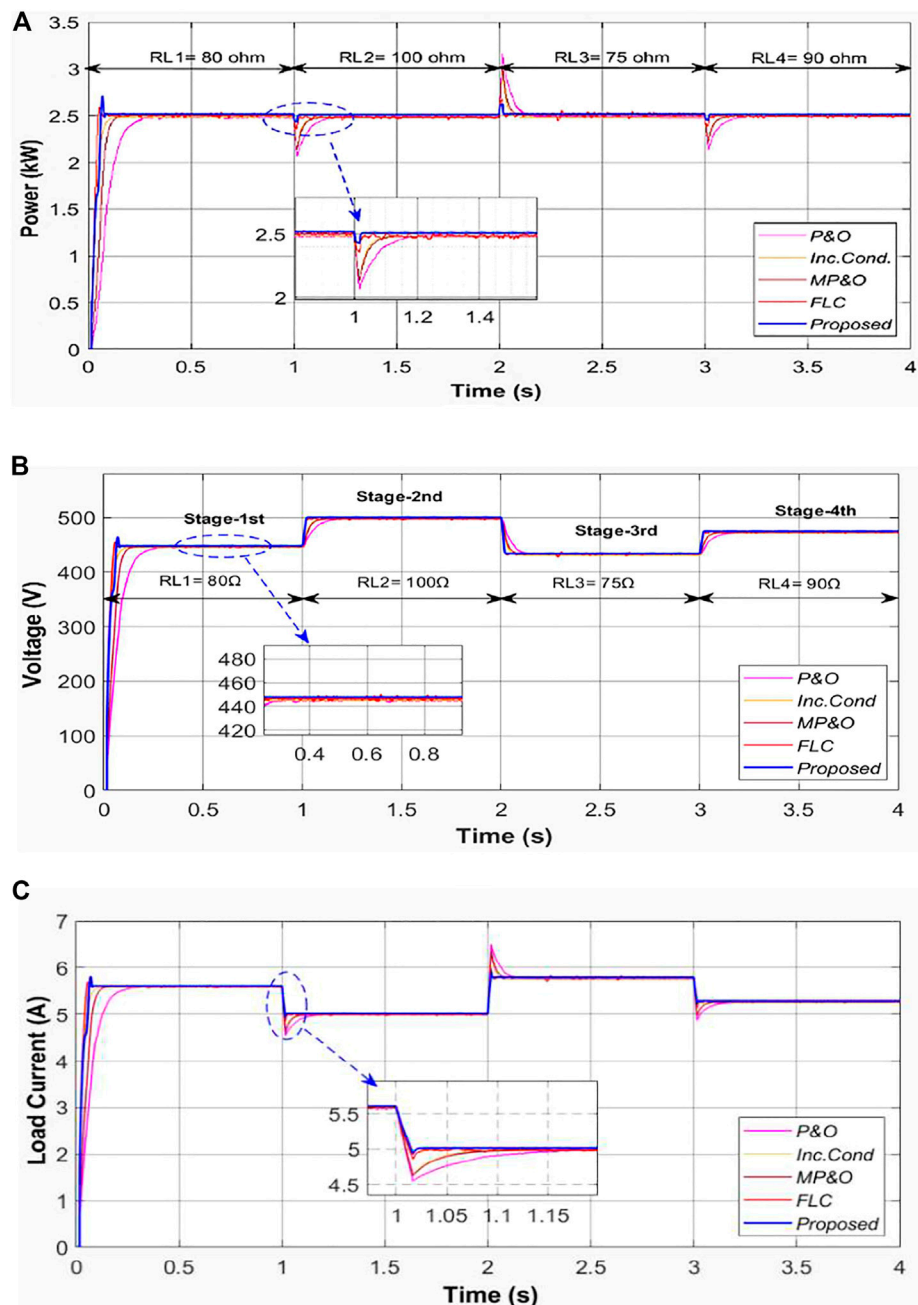


FIGURE 12 | Responses under Scenario-III: (A) Output power ( $P_0$ ) (B) output voltage ( $V_o$ ) and (C) output current ( $I_o$ )

## 4 RESULTS AND DISCUSSIONS

In order to conduct a performance analysis of the proposed adaptive A-P&O MPPT technique a 2.56 kW PV energy conversion system as depicted in **Figure 1** is considered. Performance is also compared with P&O, Inc Cond, modified P&O, and FLC MPPT techniques. The simulation results are

validated in MATLAB/Simulink using a personal computer with an Intel<sup>R</sup> Core<sup>TM</sup> i7 CPU at 2.2 GHz and 8 GB of RAM. The following three scenarios of operating conditions have been considered for the investigation:

- Scenario-I: Varying irradiance at a fixed temperature.
- Scenario-II: Varying temperature at fixed irradiance.

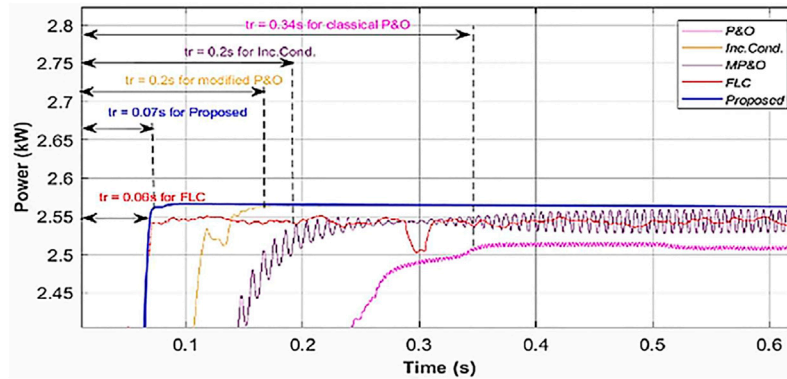


FIGURE 13 | Performance of dynamic response time ( $t_r$ ) of MPPTs tested under Scenario-I in level  $S_1$ .

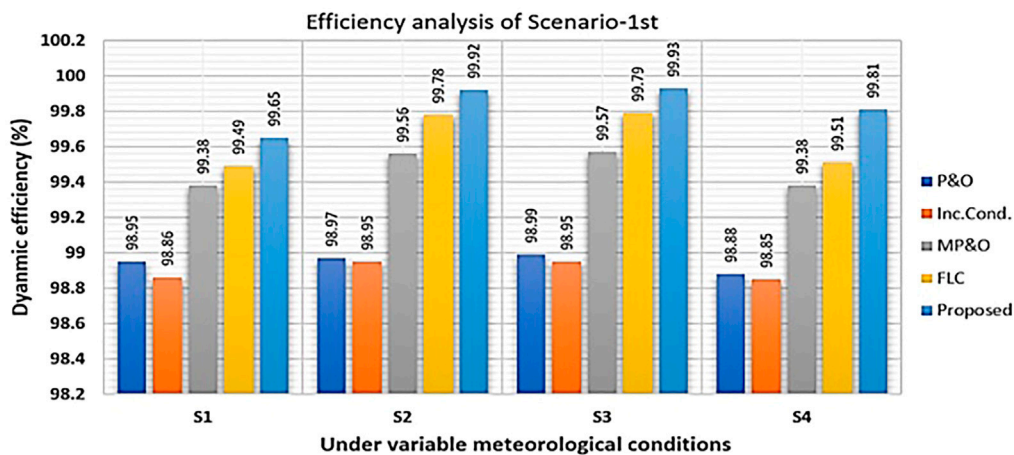


FIGURE 14 | Convergence time and dynamic efficiency under scenario-first.

- Scenario-III: Varying load at standard test condition.

#### 4.1 Scenario-I: Varying Irradiance at Constant Temperature

In this scenario, the performance investigation of the proposed MPPT technique is performed under dynamic behavior such as varying irradiance at constant ambient temperature  $T_{STC} = 25^{\circ}\text{C}$  and fixed  $R_{Load}$  at  $97.55\ \Omega$ , respectively. The simulation results are verified at varying irradiance of four levels (or stages) of  $S_{11}$ ,  $S_{12}$ ,  $S_{13}$ , and  $S_{14}$ . Figure 7 illustrates the variation pattern of irradiance with a sudden change in levels from  $S_{11}$  is  $1000\ \text{W/m}^2$  to  $750\ \text{W/m}^2$  during  $t_{rs11} = 0-0.8\ \text{s}$ ;  $S_{12}$  is  $750\ \text{W/m}^2$  to  $500\ \text{W/m}^2$  during  $t_{rs12} = 0.8-1.5\ \text{s}$ ;  $S_{13}$  is  $500\ \text{W/m}^2$  to  $1000\ \text{W/m}^2$  during  $t_{rs13} = 1.5\ \text{s}$  to  $3.0\ \text{s}$ ; and  $S_{14}$  reporting to its previous level, i.e.,  $1000\ \text{W/m}^2$  during  $t_{rs14} = 3.0-4.0\ \text{s}$ , respectively.

Theoretical values of maximum power obtainable on  $S_{11}$ ,  $S_{12}$ ,  $S_{13}$ , and  $S_{14}$  are  $2.56$ ,  $1.94$ ,  $1.28$ , and  $2.56\ \text{kW}$ , respectively.

During this scenario, power, voltage and load current behavior obtained for different MPPT techniques are illustrated in Figure 8. It is evident from the results that the proposed control technique gives the least oscillations around MPP with fast-tracking response, less power ripples, and effectively improved efficiency that is better than the other four conventional MPPT techniques.

Output power obtained, response time, and efficiency under steady-state with different MPPT techniques are tabulated in Table 3. Output power of  $P_{0,S11} = 2.55\ \text{kW}$  with output voltage  $V_{0,S11} = 501.5\ \text{V}$  and load current  $I_{0,S11} = 5.09\ \text{Amp}$  is achieved with rise time  $t_{rs11} = 39.9\ \text{m-sec}$ . It is evident from the results obtained that for all variable irradiance stages  $S_{12}$ ,  $S_{13}$ , and  $S_{14}$ , the proposed MPPT technique also gives better performance compared with the other four conventional techniques which are depicted clearly in Table 3.

## 4.2 Scenario-II: Varying Temperature at Constant Irradiance

In this scenario, the performance investigation of proposed MPPT technique is performed under the dynamic behavior such as varying temperature at constant irradiance for  $G_{STC} = 1000 \text{ W/m}^2$  and fixed  $R_{Load} = 97.55 \Omega$ , respectively. The simulation results are verified at varying irradiance of four levels (or stages) of  $S_{21}$ ,  $S_{22}$ ,  $S_{23}$ , and  $S_{24}$ . **Figure 9** illustrates that the tracking accuracy of the system under varying temperatures with sudden change levels from  $S_{21}$  is  $20^\circ\text{C}$  to  $50^\circ\text{C}$  during  $t_{rs21} = 0 \text{ s}$  to  $0.8 \text{ s}$ ;  $S_{22}$  is  $50^\circ\text{C}$  to  $30^\circ\text{C}$  during  $t_{rs22} = 0.8\text{--}1.5 \text{ s}$ ;  $S_{23}$  is  $30^\circ\text{C}$  to  $40^\circ\text{C}$  during  $t_{rs23} = 1.5 \text{ s}$  to  $2.5 \text{ s}$ ; and  $S_{24}$  reporting to its previous level, i.e.,  $40^\circ\text{C}$  during  $t_{rs24} = 2.5 \text{ s}$  to  $4.0 \text{ s}$ , respectively. The theoretical value of maximum power obtainable on  $S_{21}$ ,  $S_{22}$ ,  $S_{23}$ , and  $S_{24}$  are 2.62, 2.26, 2.50, and 2.38 kW, respectively.

During this scenario, all the levels of power, voltage and load current are tracked successfully using a boost converter for variable scaling factors as shown in **Figure 9** and **Figures 10A–C**. The proposed control technique gives the least oscillations around MPP with fast-tracking response, less power, ripples, and effective improved efficiency are better than the other four conventional MPPT techniques as shown in **Table 4**. Accordingly, **Figure 10A**, **Figure 10B**, **Figure 10C** and **Table 4** illustrates that the proposed control technique (blue) gives output power ( $P_{o,S21}$ ) = 2.612 kW, output voltage ( $V_{o,S21}$ ) = 508.5 V and load current ( $I_{o,S21}$ ) = 5.12 Amp settled at  $t_{rs21} = 39.1 \text{ m-sec}$  as compared with other four conventional P&O (pink); Inc Cond (yellow); MP&O (brown) and FLC (red) based MPPT techniques, respectively. That is approximately identical to ideal values  $P_{m,S21}$  in PV array operated at temperature  $S_{21} = 20^\circ\text{C}$ , more detailed as depicted in **Table 6**. Similarly, for all variable temperature stages  $S_{22}$ ,  $S_{23}$ , and  $S_{24}$  the proposed MPPT technique also gives better performance as compared to the other four conventional techniques which are depicted clearly in **Table 4**.

## 4.3 Scenario-III: Varying Load at Standard Test Condition

In this scenario, the performance comparison analysis of proposed MPPT technique is performed under dynamic behavior such as varying load at constant irradiance,  $G_{STC}$  is  $1000 \text{ W/m}^2$  and constant  $T_{STC}$  is  $25^\circ\text{C}$ , respectively. The simulation results are verified at varying load resistance of four levels (or stages) of  $S_{31}$ ,  $S_{32}$ ,  $S_{33}$ , and  $S_{34}$ . Similarly, **Figure 11** illustrates the tracking accuracy of the system under varying resistive load with sudden change levels from  $S_{31} = 80 \Omega$  during  $t_{rs31} = 0 \text{ s}$  to  $1.0 \text{ s}$ ;  $S_{32} = 100 \Omega$  during  $t_{rs32} = 1.0 \text{ s}$  to  $2.0 \text{ s}$ ;  $S_{33} = 75 \Omega$  during  $t_{rs33} = 2.0\text{--}3.0 \text{ s}$ ; and  $S_{34}$  reporting to its previous level i.e.,  $90 \Omega$  during  $t_{rs34} = 3.0\text{--}4.0 \text{ s}$ , respectively. The theoretical value of maximum power obtainable on  $S_{31}$ ,  $S_{32}$ ,  $S_{33}$ , and  $S_{34}$  is 2.56 kW.

During this scenario, all the levels of power, voltage, and load current are tracked successfully by employing a boost converter for variable scaling factors as shown in **Figures 12A–C**. Accordingly, **Figure 12A**, **Figure 12B**, **Figure 12C** and **Table 5** illustrates that the proposed control technique (blue) gives output power  $P_{o,S31} =$

2.553 kW, output voltage  $V_{o,S31} = 451.4 \text{ V}$  and load current  $I_{o,S31} = 5.67 \text{ Amp}$  settled at  $t_{rs31} = 39.9 \text{ m-sec}$  as compared with other four conventional P&O (pink); Inc Cond (yellow); MP&O (brown) and FLC (red) based MPPT techniques, approximately identical to ideal values  $P_{m,S31}$  in PV array operated at load resistance  $S_{31} = 80 \Omega$ . Similarly, for all load resistance stages  $S_{32}$ ,  $S_{33}$ , and  $S_{34}$  the proposed MPPT technique gives better performance as compared with the other four conventional techniques which are depicted clearly in **Table 5**.

## 4.4 Transient State Analysis

To verify the performances of all five considered MPPT techniques investigated during the transient state, responses of the PV system under scenario-I for level  $S_{11}$  are recorded. Responses obtained are shown in **Figure 13**. The sampling time captured in Scenario-I for level  $S_{11}$  for proposed MPPT technique is 35.8 m-sec., for P&O is 301 m-sec, for Inc Cond is 121 m-sec., for MP&O is 200 m-sec., and for FLC is 40 m-sec, respectively.

The proposed technique tested under standard test conditions ( $G_{STC}$  is  $1000 \text{ W/m}^2$  and  $T_{STC}$  is  $25^\circ\text{C}$ ) achieved dynamic efficiency of 99.68% which is better than the other four conventional control techniques as shown in **Figure 14**.

Overall performance comparison analysis of tracking simulation results is validated for the proposed and conventional MPPTs under all three different scenarios and given in **Table 6**. From **Table 6**, it is evident that proposed technique is better than other conventional techniques available in the literature. The proposed technique gives better efficiency, more output power, and lesser ripple in comparison to other techniques.

## 5 CONCLUSION

In this paper, an improved P&O MPPT technique is proposed and developed with a mechanism to automatically adjust the step-size, possessing the characteristics of accurate rapid tracking response, effectively improved efficiency, reducing oscillations, and extracting optimal power for PV energy conversion system. The performance of the developed adaptive step-sized MPPT algorithm is compared with the other four conventional MPPT techniques; such as P&O, I&C, modified P&O, and FLC-based techniques. Performance validation is conducted under sudden changes of meteorological conditions and load variations considering the steady-state and dynamic conditions. The developed algorithm is tested for a 2.563 kW PV energy conversion system, using MATLAB/Simulink environment under varying irradiance, varying ambient temperatures, and varying load conditions. The effective efficiency of PV system using the developed adaptive step-sized MPPT algorithm improves from 99.61 to 99.9%, as compared to the other four conventional MPPT techniques. In terms of accuracy, the FLC MPPT algorithm comes closer to the developed algorithm but the adaptive step-size MPPT algorithm performs better in terms of tracking accuracy and limiting the oscillations. The proposed improved adaptive step-size P&O MPPT algorithm finds its

applications in tracking the maximum power under sudden changes in the ambient environmental conditions. In the future, the developed algorithm can be realized experimentally in order to further improve its applicability by incorporating more realistic working conditions

## DATA AVAILABILITY STATEMENT

The raw data supporting the conclusion of this article will be made available by the authors, without undue reservation.

## REFERENCES

- Abo-Al-Ez, K. M., Kaddah, S. S., Diab, S., and Abdraboh, E.-H. (2020). Performance Analysis of Maximum Power Point Tracking (MPPT) for PV Systems under Real Meteorological Conditions. *Green Energy Technol.* 199–228. doi:10.1007/978-3-030-05578-3\_7
- Ahmed, J., and Salam, Z. (2016). A Modified P&O Maximum Power Point Tracking Method with Reduced Steady-State Oscillation and Improved Tracking Efficiency. *IEEE Trans. Sustain. Energy* 7 (4), 1506–1515. doi:10.1109/TSTE.2016.2568043
- Algarín, C. R., Giraldo, J. T., and Álvarez, O. R. (2017). Fuzzy Logic Based MPPT Controller for a PV System. *Energies* 10 (12), 2036. doi:10.3390/en10122036
- Ali, A. I. M., Sayed, M. A., and Mohamed, E. E. M. (2018). Modified Efficient Perturb and Observe Maximum Power Point Tracking Technique for Grid-Tied PV System. *Int. J. Electr. Power & Energy Syst.* 99, 192–202. doi:10.1016/j.ijepes.2017.12.029
- Ali, M. M., Youssef, A. R., Ali, A. S., and Abdel-Jaber, G. T. (2020). Variable Step Size PO MPPT Algorithm Using Model Reference Adaptive Control for Optimal Power Extraction. *Int. Trans. Electr. Energy Syst.* 30 (1), 1–21. doi:10.1002/2050-7038.12151
- Amara, K., Fekik, A., Hocine, D., Bakir, M. L., Bourennane, E.-B., Malek, T. A., et al. (2018). “Improved Performance of a PV Solar Panel with Adaptive Neuro Fuzzy Inference System ANFIS Based MPPT,” in Proceeding of the 7th International IEEE Conference on Renewable Energy Research and Applications, ICRERA 2018, Paris, France, Oct. 2018 (IEEE), 1098–1101. 5. doi:10.1109/ICRERA.2018.8566818
- Amir, A., Amir, A., Selvaraj, J., Rahim, N. A., and Abusorrah, A. M. (2017). Conventional and Modified MPPT Techniques with Direct Control and Dual Scaled Adaptive Step-Size. *Sol. Energy* 157 (August), 1017–1031. doi:10.1016/j.solener.2017.09.004
- Amir, M., and Srivastava, S. K. (2018). “Analysis of MPPT Based Grid Connected Hybrid Renewable Energy System with Battery Backup,” in Proceeding of the 2018 International Conference on Computing, Power and Communication Technologies, GUCON 2018, Greater Noida, India, Sept. 2018 (IEEE), 903–907. doi:10.1109/GUCON.2018.8674902
- Aouchiche, N., Aitcheikh, M. S., Becherif, M., and Ebrahim, M. A. (2018). AI-based Global MPPT for Partial Shaded Grid Connected PV Plant via MFO Approach. *Sol. Energy* 171 (June), 593–603. doi:10.1016/j.solener.2018.06.109
- Bayrak, G., and Ghaderi, D. (2019). An Improved Step-up Converter with a Developed Real-time Fuzzy-based MPPT Controller for PV-based Residential Applications. *Int. Trans. Electr. Energy Syst.* 29 (12), 1–20. doi:10.1002/2050-7038.12140
- Ben Salah, C., and Ouali, M. (2011). Comparison of Fuzzy Logic and Neural Network in Maximum Power Point Tracker for PV Systems. *Electr. Power Syst. Res.* 81 (1), 43–50. doi:10.1016/j.epr.2010.07.005
- Bendib, B., Belmili, H., and Krim, F. (2015). A Survey of the Most Used MPPT Methods: Conventional and Advanced Algorithms Applied for Photovoltaic Systems. *Renew. Sustain. Energy Rev.* 45, 637–648. doi:10.1016/j.rser.2015.02.009
- Chauhan, U., Rani, A., Singh, V., and Kumar, B. (2020). “A Modified Incremental Conductance Maximum Power Point Technique for Standalone PV System,” in Proceeding of the 2020 7th International Conference on Signal Processing and Integrated Networks, SPIN, Noida, India, Feb. 2020 (IEEE), 61–64. doi:10.1109/SPIN48934.2020.9071156
- Derbeli, M., Napole, C., Barambones, O., Sanchez, J., Calvo, I., and Fernández-Bustamante, P. (2021). Maximum Power Point Tracking Techniques for Photovoltaic Panel: A Review and Experimental Applications. *Energies* 14 (22), 7806–7831. doi:10.3390/en14227806
- Dolara, A., Faranda, R., and Leva, S. (2009). Energy Comparison of Seven MPPT Techniques for PV Systems. *J. Electromagn. Analysis Appl.* 01 (03), 152–162. doi:10.4236/jemaa.2009.13024
- Elbaset, A., Ali, H., and Abd-El Sattar, M. (2015). A Modified Perturb and Observe Algorithm for Maximum Power Point Tracking of Photovoltaic System Using Buck-Boost Converter. *JES. J. Eng. Sci.* 43, 344–362. Sciences Assiut University Faculty of Engineering. doi:10.21608/jesau.2015.115189
- Eltamaly, A. M., and Farh, H. M. H. (2019). Dynamic Global Maximum Power Point Tracking of the PV Systems under Variant Partial Shading Using Hybrid GWO-FLC. *Sol. Energy* 177, 306–316. doi:10.1016/j.solener.2018.11.028
- Esrām, T., and Chapman, P. L. (2007). Comparison of Photovoltaic Array Maximum Power Point Tracking Techniques. *IEEE Trans. Energy Convers.* 22 (2), 439–449. doi:10.1109/TEC.2006.874230
- Hlaili, M., and Mechergui, H. (2016). Comparison of Different MPPT Algorithms with a Proposed One Using a Power Estimator for Grid Connected PV Systems. *Int. J. Photoenergy* 2016, 1–10. doi:10.1155/2016/1728398
- Jana, S., Kumar, N., Mishra, R., Sen, D., and Saha, T. K. (2020). Development and Implementation of Modified MPPT Algorithm for Boost Converter-based PV System under Input and Load Deviation. *Int. Trans. Electr. Energy Syst.* 30 (2), 1–15. doi:10.1002/2050-7038.12190
- Jiayi, H., Chuanwen, J., and Rong, X. (2008). A Review on Distributed Energy Resources and MicroGrid. *Renew. Sustain. Energy Rev.* 12 (9), 2472–2483. doi:10.1016/j.rser.2007.06.004
- Jordehi, A. R. (2016). Maximum Power Point Tracking in Photovoltaic (PV) Systems: A Review of Different Approaches. *Renew. Sustain. Energy Rev.* 65, 1127–1138. doi:10.1016/j.rser.2016.07.053
- Kottas, T. L., Boutalis, Y. S., and Karlis, A. D. (2006). New Maximum Power Point Tracker for PV Arrays Using Fuzzy Controller in Close Cooperation with Fuzzy Cognitive Networks. *IEEE Trans. Energy Convers.* 21 (3), 793–803. doi:10.1109/TEC.2006.875430
- Kumar, B., Chauhan, Y. K., and Shrivastava, V. (2014). A Comparative Study of Maximum Power Point Tracking Methods for a Photovoltaic-Based Water Pumping System. *Int. J. Sustain. Energy* 33 (4), 797–810. doi:10.1080/14786451.2013.769990
- Li, S. (2019). A Variable-Weather-Parameter MPPT Control Strategy Based on MPPT Constraint Conditions of PV System with Inverter. *Energy Convers. Manag.* 197 (February), 111873. doi:10.1016/j.enconman.2019.111873
- Li, J., and Wang, H. (2009). “A Novel Stand-Alone PV Generation System Based on Variable Step Size INC MPPT and SVPWM Control,” in Proceeding of the 2009 IEEE 6th International Power Electronics and Motion Control Conference, IPEMC '09, Wuhan, China, May 2009 (IEEE), 2155–2160. 3. doi:10.1109/IPEMC.2009.5157758
- Loukil, K., Abbes, H., Abid, H., Abid, M., and Toumi, A. (2020). Design and Implementation of Reconfigurable MPPT Fuzzy Controller for Photovoltaic Systems. *Ain Shams Eng. J.* 11, 319–328. doi:10.1016/j.asej.2019.10.002

## AUTHOR CONTRIBUTIONS

All authors listed have made a substantial, direct, and intellectual contribution to the work and approved it for publication.

## FUNDING

This research received no specific grant from any funding agency in the public, commercial, or not-for-profit sectors.

- Mamarelis, E., Petrone, G., and Spagnuolo, G. (2014). Design of a Sliding-Mode-Controlled SEPIC for PV MPPT Applications. *IEEE Trans. Ind. Electron.* 61 (7), 3387–3398. doi:10.1109/TIE.2013.2279361
- Mekhilef, S., Saidur, R., and Safari, A. (2011). A Review on Solar Energy Use in Industries. *Renew. Sustain. Energy Rev.* 15 (4), 1777–1790. doi:10.1016/j.rser.2010.12.018
- Mousa, H. H. H., Youssef, A.-R., and Mohamed, E. E. M. (2021). State of the Art Perturb and Observe MPPT Algorithms Based Wind Energy Conversion Systems: A Technology Review. *Int. J. Electr. Power & Energy Syst.* 126, 106598. doi:10.1016/j.ijepes.2020.106598
- Pavithra, C., Singh, P., Sundramurthy, V. P., Karthik, T. S., Karthikeyan, P. R., T. Abraham, J., et al. (2021). “A Brief Overview of Maximum Power Point Tracking Algorithm for Solar PV System,” in *Materials Today: Proceedings* (Elsevier), 10–13. doi:10.1016/j.matpr.2021.01.220
- Reza Reisi, A., Hassan Moradi, M., and Jamasb, S. (2013). Classification and Comparison of Maximum Power Point Tracking Techniques for Photovoltaic System: A Review. *Renew. Sustain. Energy Rev.* 19, 433–443. doi:10.1016/j.rser.2012.11.052
- Safari, A., and Mekhilef, S. (2011). Simulation and Hardware Implementation of Incremental Conductance MPPT with Direct Control Method Using Cuk Converter. *IEEE Trans. Ind. Electron.* 58 (4), 1154–1161. doi:10.1109/TIE.2010.2048834
- Saravanan, S., and Ramesh Babu, N. (2016). Maximum Power Point Tracking Algorithms for Photovoltaic System - A Review. *Renew. Sustain. Energy Rev.* 57, 192–204. doi:10.1016/j.rser.2015.12.105
- Wang, N., Jin, M., Wang, Z., and Cheng, M. (2018). “Optimization of Photovoltaic MPPT System Efficiency Based on Combined Algorithm,” in *Proceeding of the ICEMS 2018 - 2018 21st International Conference on Electrical Machines and Systems, Jeju, Korea, Oct. 2018 (Jeju (South Korea): KIEE EMECS KIEE Electrical Machinery and Energy Conversion Systems)*, 1122–1126. doi:10.23919/ICEMS.2018.8549191
- Yilmaz, U., Turksoy, O., and Teke, A. (2019). Improved MPPT Method to Increase Accuracy and Speed in Photovoltaic Systems under Variable Atmospheric Conditions. *Int. J. Electr. Power & Energy Syst.* 113 (May), 634–651. doi:10.1016/j.ijepes.2019.05.074
- Conflict of Interest:** The authors declare that the research was conducted in the absence of any commercial or financial relationships that could be construed as a potential conflict of interest.
- Publisher’s Note:** All claims expressed in this article are solely those of the authors and do not necessarily represent those of their affiliated organizations, or those of the publisher, the editors, and the reviewers. Any product that may be evaluated in this article, or claim that may be made by its manufacturer, is not guaranteed or endorsed by the publisher.
- Copyright © 2022 Singh, Singh, Verma and Kumar. This is an open-access article distributed under the terms of the Creative Commons Attribution License (CC BY). The use, distribution or reproduction in other forums is permitted, provided the original author(s) and the copyright owner(s) are credited and that the original publication in this journal is cited, in accordance with accepted academic practice. No use, distribution or reproduction is permitted which does not comply with these terms.